HHS Public Access

Author manuscript

J Magn Reson Imaging. Author manuscript; available in PMC 2018 October 01.

Published in final edited form as:

J Magn Reson Imaging. 2017 October ; 46(4): 1045–1052. doi:10.1002/jmri.25653.

Simultaneous non-contrast angiography and intraplaque hemorrhage (SNAP) imaging:

Comparison with contrast-enhanced MR angiography for measuring carotid stenosis

Hongge Shu, MD[1,2], **Jie Sun, MD**[2], **Thomas S. Hatsukami, MD**[3], **Niranjan Balu, PhD**[2], **Daniel S. Hippe, MS**[2], **Haining Liu, MS**[4], **Ted R. Kohler, MD**[3,5], **Wenzhen Zhu, MD**[1], and **Chun Yuan, PhD**[2,4]

[1]Department of Radiology, Tongji Hospital, Huazhong University of Science and Technology, Wuhan, China

[2]Department of Radiology, University of Washington, Seattle, WA, U.S

[3]Department of Surgery, University of Washington, Seattle, WA, U.S

[4]Department of Bioengineering, University of Washington, Seattle, WA, U.S

[5]Surgery and Perioperative Care, VA Puget Sound Health Care System, Seattle, WA, U.S

Abstract

Purpose—There is a growing interest in detecting intraplaque hemorrhage (IPH) during the clinical management of carotid disease, yet luminal stenosis has remained indispensable during clinical decision-making. Simultaneous Non-contrast Angiography and intraPlaque hemorrhage (SNAP) imaging has been proposed as a novel IPH imaging technique that provides carotid MR angiography (MRA) with no added scan time. Flowing blood shows negative signal on SNAP because of phase-sensitive inversion recovery. In a proof-of-concept study, we evaluated the feasibility of SNAP as a clinical MRA technique for measuring carotid stenosis.

Materials and Methods—58 asymptomatic subjects with 16–79% stenosis on ultrasound were scanned at 3T by SNAP with 0.8 mm isotropic resolution and 16 cm longitudinal coverage. Two readers measured luminal stenosis of bilateral carotid arteries (n=116) on minimum intensity projections of SNAP using the NASCET criteria. In the subset (48 arteries) with contrast-enhanced (CE) MRA available for comparison, luminal stenosis was also measured on maximum intensity projections of CE-MRA.

Results—Intra-class correlation coefficients (ICCs) with 95% confidence intervals were 0.94 (0.90–0.96) and 0.93 (0.88–0.96) for intra- and inter-reader agreement on stenosis measurements, respectively. Corresponding kappas for grading stenosis (0–29%, 30–69%, 70–99%, and 100%) were 0.79 (0.67–0.89) and 0.80 (0.68–0.90). Agreement between SNAP and CE-MRA was high (ICC: 0.95 [0.90–0.98]; kappa: 0.82 [0.71–0.93]).

Conclusion—As a dedicated IPH-imaging sequence, SNAP also provided carotid stenosis measurement that showed high intra- and inter-reader consistency and excellent agreement with

Correspondence: Jie Sun, MD, 850 Republican St Rm 127, Seattle, WA 98109, Tel: +1-206-685-2231, Fax: +1-206-616-9354, sunjie@uw.edu.

CE-MRA. Further comparisons with digital subtraction angiography and other noninvasive techniques are warranted.

Keywords

carotid disease; magnetic resonance angiography; NASCET; intraplaque hemorrhage

INTRODUCTION

In the clinical management of carotid disease, considerable attention has recently been directed to intraplaque hemorrhage (IPH), which is recognized as a hallmark feature that may alter the biology and natural history of carotid atherosclerosis (1–3). As a strong predictor for ipsilateral cerebrovascular events (4, 5), imaging IPH is expected to contribute to more effective primary and secondary prevention of ischemic stroke if such information is properly incorporated into clinical practice (6). In patients presenting with new-onset ischemic symptoms, imaging IPH can help determine the etiology, particularly in the presence of low-grade luminal stenosis (7).

Although various imaging modalities are used clinically for evaluating carotid disease, magnetic resonance imaging (MRI) is the only one that has achieved in vivo IPH detection (8–10). Dedicated IPH-imaging techniques typically do not provide stenosis measurements. Therefore, a separate MR angiography (MRA) is required to measure luminal stenosis because of its wide use in patient triage in previous and ongoing clinical trials (11–13). In this context, Simultaneous Non-contrast Angiography and intraPlaque hemorrhage (SNAP) imaging was proposed (14), which may facilitate the translation of IPH imaging from research to clinical practice by allowing for concurrent evaluation of luminal stenosis. However, the feasibility of SNAP for measuring carotid stenosis according to the North American Symptomatic Carotid Endarterectomy Trial (NASCET) criteria (11, 12), which is considered the clinical standard, has not been evaluated. As a non-contrast MRA technique, the robustness of SNAP in handling slow or turbulent flow needs to be tested against conventional contrast-enhanced (CE) MRA (15, 16). Thus, this study sought to evaluate the feasibility of SNAP as a clinical MRA approach for measuring carotid stenosis.

MATERIALS AND METHODS

Study Sample

All study procedures were approved by the institutional review board. Written informed consent was obtained prior to study for all subjects. Subjects were recruited as part of an ongoing prospective cohort study that examines the natural history of carotid atherosclerosis (17). Patients aged 50–85 years, free from cerebrovascular events within the past 6 months, and with 16–79% stenosis by duplex ultrasound in at least one carotid artery were recruited. Exclusion criteria included prior history of radiation therapy to the neck, autoimmune arteritis, recent cardiovascular events, and contraindications for MR examination or contrast injection (e.g. claustrophobia, metal implant, and estimated glomerular filtration rate <60 ml/min/1.73m^2). A screening black-blood MRI (25 cm longitudinal coverage) was

performed (18, 19). All subjects with distinct plaque(s) (maximum wall thickness≥2 mm) in at least one carotid artery were consecutively enrolled.

MRI Examination: SNAP And CE-MRA

All MR scans were performed on a 3T whole-body scanner (Philips Healthcare, Best, the Netherlands). SNAP was acquired using an eight-channel phased-array surface coil (Chenguang Medical Technologies, Shanghai, China) placed around the neck whereas CE-MRA was acquired using either the surface coil or body coil. The design of the SNAP sequence has been previously reported (14). In SNAP imaging, inversion-recovery pulses are applied axially to a large slab, followed by phase-sensitive acquisition in a limited coronal slab. Inflowing blood experiences the inversion pre-pulse once before image acquisition, and only once before flowing out of the imaging slab. Because of the inversion pre-pulse and phase-sensitive reconstruction (14), IPH has highly positive signal, vessel wall has intermediate signal, and flowing blood has highly negative signal on SNAP (Figure 1). Acquisition was in the coronal plane with repetition time=10 ms, echo time=4.8 ms, flip angle=11°, inversion time=500 ms, inversion recovery repetitive time=1970 ms, field-of-view=160×160×32 mm^2, number of excitations=2. Resolution was 0.8×0.8×0.8 mm^2 acquired and 0.4×0.4×0.4 mm^2 interpolated. Scan time was 5 minutes 17 seconds. In subjects agreed to undergo CE-MRA, first-pass CE-MRA was performed using a three-dimensional spoiled gradient-echo sequence with bolus timing. Acquisition was in coronal plane with repetition time=5.5 ms, echo time=1.7 ms, flip angle=30°, field-of-view=350×350×64 mm^2, number of excitations=1. Spatial resolution was the same as SNAP. The sequence was performed before (the mask) and after intravenous infusion of 0.1 mmol/kg gadopentetate dimeglumine (Magnevist, Bayer Healthcare, Wayne, NJ) by a power injector at a rate of 2 ml/s followed by 20 ml of saline (Figure 1). Total scan time for CE-MRA was about 6–7 minutes.

Image Analysis

Standardized post-processing was performed at the MR console to generate 18 radially projected angiograms at 10° increments for both SNAP and CE-MRA so that the projection showing maximum stenosis could be readily identified during subsequent, blinded review. For CE-MRA, the pre-contrast data set was subtracted from the post-contrast data set to eliminate background signals. The subtracted data set was then used to generate maximum intensity projection (MIP) images. Each carotid artery was segmented manually and saved separately for offline review (Figure 1). For SNAP, the phase-sensitive reconstruction algorithm automatically generated a new data set after scanning by combining magnitude and phase information. This data set was identified and used to generate minimum intensity projection (mIP) images (Figure 1). Each carotid artery was segmented manually to remove any interfering venous structures and saved separately for offline review.

Identifying information was removed and images were randomized. Two readers (H.S. and J.S.), with 10 and 6 years of experience in MRI, independently measured carotid stenosis on SNAP mIP images accordingly to the NASCET criteria (11, 20). The projection that demonstrated the most severe narrowing was identified. Two measurements were made: 1)

luminal diameter at the site of maximal narrowing; 2) luminal diameter of the normal distal internal carotid artery beyond the bulb where artery walls become parallel.

Carotid stenosis was calculated as (1 − *minimum luminal diameter/normal reference diameter*) × 100%. Severe stenosis was considered and recorded as 99% in the presence of: 1) signal void with a distal patent artery or 2) the string sign associated with near occlusion (21). Total occlusion without distal flow was recorded as 100%. Source images were also available during image review and axial reformats were referred to as necessary to confirm the signal polarity of a particular area. One month after SNAP review, one reader (J.S.) analyzed CE-MRA images blinded to SNAP results in the same fashion. The other reader (H.S.) re-analyzed SNAP images blinded to previous reading results to estimate intra-reader consistency.

Statistical Analysis

Quantitative measurements were evaluated using the intra-class correlation coefficient (ICC; absolute agreement assessed with two-way random effects model). Additionally, measurements were categorized as no or mild stenosis (0–29%), moderate stenosis (30–69%), severe stenosis (70–99%), or total occlusion (100%) (20, 22), and evaluated using Cohen's weighted kappa (linear weights). The non-parametric bootstrap and percentile method was used to calculate 95% confidence intervals for ICC and kappa estimates, with resampling performed by subject to account for any dependence between arteries from the same subject (23). Statistical calculations were conducted with SPSS (version 17.0, SPSS Inc., Chicago, IL) and R (version 3.1.1, R Foundation for Statistical Computing, Vienna, Austria).

RESULTS

Fifty-eight subjects with distinct carotid plaque were enrolled (Table 1). Of the 116 carotid arteries imaged using SNAP, stenosis was not measured due to poor image quality or insufficient coverage in 6 (5.2%) arteries in the first reading session by Reader 1, in 8 (6.9%) arteries in the second reading session by Reader 1, and in 5 (4.3%) arteries in the reading session by Reader 2. Insufficient coverage was noted when a portion of carotid plaque was not within the scan field, which in this study only affected lesions in the common carotid artery in cases with a low carotid bifurcation.

Based on measurements on SNAP MRA (one of the three readings), carotid stenosis ranged from 0% to 100% in this population with a mean value of 28±26%. Sixty-seven (60%) had no or mild stenosis (0–29%), 38 (34%) had moderate stenosis (30–69%), 5 (5%) had severe stenosis (70–99%), and 1 (1%) had total occlusion (100%). Quantitative stenosis measurements on SNAP MRA demonstrated high reader consistency, with an ICC of 0.94 (0.90–0.96) for intra-reader consistency (first SNAP reading by Reader 1 versus second SNAP reading by Reader 1) and an ICC of 0.93 (0.88–0.96) for inter-reader consistency (first SNAP reading by Reader 1 versus SNAP reading by Reader 2) (Figure 2). The corresponding kappa values were 0.79 (0.67–0.89) and 0.80 (0.68–0.90). For both intra- and inter-reader comparison, some arteries were measured in one reading session but not the other. Most of these discrepant cases had <30% stenosis when measured, which are more

likely to be missed compared to more stenotic arteries when mIP projections are screened for stenosis.

MIP images were reconstructed for 48 carotid arteries where CE-MRA data were available for comparison. Carotid stenosis of the 48 arteries ranged from 0% to 100% (mean value: 30±27%). Quantitative stenosis measurements on SNAP and CE-MRA demonstrated a high agreement with an ICC of 0.95 (0.91–0.98) (SNAP reading by Reader 2 versus CE-MRA reading by Reader 2) (Figure 3). The Bland-Altman plot shows a small mean difference and there was no apparent relationship between the difference and mean of stenosis measurements (Figure 3). Lumen boundaries were mostly conspicuous on SNAP MRA when signal-to-noise was sufficient, including regions downstream to stenosis where turbulent flow is speculated (Figure 4). Both total occlusion and near occlusion on CE-MRA were similarly identified on SNAP MRA (Figure 5). Stenosis grading agreed between SNAP MRA and CE-MRA in 42 (87.5%) arteries, yielding a weighted kappa of 0.82 (0.71–0.93) (Table 2).

DISCUSSION

This study evaluated the potential clinical utility of SNAP as a non-contrast MRA technique for measuring carotid stenosis. Large-coverage angiograms can be generated using mIP reconstruction of SNAP data to facilitate the use of the NASCET criteria in a similar manner to MIP reconstruction of CE-MRA data. Intra- and inter-reader consistency on measuring carotid stenosis were high, which was attributed to the satisfactory image quality and conspicuous lumen boundaries on SNAP. Importantly, luminal stenosis measured on SNAP was highly consistent with that measured on CE-MRA, which has an established role in the clinical setting. Collectively, our data demonstrate the potential of SNAP as a non-contrast carotid MRA technique. The dual capability of characterizing luminal stenosis and IPH within a single large-coverage three-dimensional scan may facilitate the clinical use of SNAP, which may address some of the emerging needs of evaluating carotid disease, including looking beyond the lumen in clinical decision-making and avoiding gadolinium contrast in patients with impaired renal function or allergies.

Although non-invasive imaging has largely replaced intra-arterial angiography for assessment of carotid disease, the choice between different non-invasive imaging modalities varies across centers. The unique capability of MRI for detecting IPH may improve its diagnostic yield. Indeed, the strong and incremental predictive value of IPH over luminal stenosis for future ischemic events could make IPH imaging a cost-effective strategy in clinical practice (24). However, information on luminal stenosis is expected to remain indispensable as it has been used in patient triage in previous and ongoing clinical trials (11, 12). Characterizing luminal stenosis and IPH in a single scan would reduce scan time and improve coregistration of IPH signals and luminal narrowing, which may facilitate the translation of IPH imaging into clinical practice.

SNAP provides one such possibility by using inversion-recovery gradient echo and phase-sensitive reconstruction (14). High contrast between vessel wall and flowing blood is concurrently achieved without affecting the high contrast between IPH and vessel wall,

which is critical for quantitative assessment of IPH signals for monitoring IPH progression (2, 3). One observation in this study was the conspicuous lumen boundaries on SNAP seen on both mIP and source images (Figure 4). As flow velocity is expected to gradually decrease from the center to peripheral regions, the sharp lumen margins indicate that blood flow with a wide range of velocities can be visualized on SNAP MRA. Further evidence was found in an extreme case with tight stenosis and near occlusion (Figure 5), where extremely slow flow is expected. Another challenging flow pattern in carotid disease is turbulent or disturbed flow, which is typically seen in the carotid bulb or downstream from a stenosis. SNAP also appeared to produce a good MRA effect in these challenging regions. The robustness of SNAP MRA in the presence of slow or turbulent flow is thought to be related to the long interval (about 2 seconds) between adjacent inversion pulses, which provides sufficient time for blood replenishment within the field-of-view. However, it should be noted that just like other MRA techniques, SNAP is not immune to intra-voxel dephasing, which may cause signal loss in the presence of turbulent flow. When lumen contrast is decreased on SNAP MRA, signal polarity information available on the source images can provide helpful information. Because of the large excitation slab (largest possible), inflowing blood experiences the inversion pre-pulse once and only once before image acquisition, which is a premise for the MRA effect of SNAP. In the rare cases that inflowing blood does not experience the inversion pre-pulse (i.e. extremely fast blood flow), it will show as high signals. Such flow artifacts, if present, should be limited to the proximal common carotid artery and rarely affect measuring carotid stenosis.

The overall agreement between SNAP and CE-MRA gave an ICC of 0.95 (0.91, 0.98) for quantitative measurement and a weighted kappa of 0.82 (0.71, 0.93) for categorical measurement of carotid stenosis. Previous studies evaluating inter-technique agreement in quantitative stenosis measurement often used Pearson's correlation coefficient, which provides an evaluation of the consistency but not absolute agreement between techniques. For instance, Nederkoorn et al (25) reported Pearson's correlation coefficients of 0.94 for CE-MRA versus digital subtraction angiography (DSA) and 0.93–0.94 for CE-MRA versus 3D time-of-flight. U-King-Im et al (26) reported a Pearson's correlation coefficient of 0.96, an ICC of 0.98 (0.97, 0.98), and a kappa of 0.73 (0.67, 0.79) for the agreement between CE-MRA and DSA. Despite some differences in statistical methods, our results were generally in line with previous studies, supporting a high agreement between SNAP and CE-MRA in measuring carotid stenosis.

Beyond IPH detection and the unique contrast mechanism, there are several other considerations in using SNAP as a non-contrast carotid MRA technique. SNAP acquisition was in the coronal plane, which allows for relatively large anatomic coverage within clinically acceptable scan times. The current coverage of 16 cm is larger than routine time-of-flight MRA and appears to be sufficient for assessment of internal carotid stenosis. The bifurcation region and distal reference segment could always be identified within the field-of-view in this study. The scan time with full k-space sampling is currently 5.3 minutes, which can be further reduced if parallel imaging is applied. Standardized post-processing is necessary in SNAP MRA, which is similar to CE-MRA and without the need to generate curved multi-planar reformats as in magnitude-only black-blood imaging (19). Complex, time-consuming post-processing is undesired in the clinical setting and may compromise

reader consistency. However, veins were not suppressed with the current SNAP sequence and needed to be cropped during mIP reconstruction. Further efforts are warranted to saturate venous signals in SNAP imaging.

This is a proof-of-concept study and limited by the asymptomatic population and a small number of severe stenosis cases. The parent study enrolled such subjects for monitoring plaque progression, and those with severe stenosis were typically not enrolled. Nonetheless, our results demonstrated the feasibility of SNAP MRA for obtaining quantitative stenosis measurements. Future studies enrolling more surgery candidates are now warranted to further assess its performance in different populations. Another limitation was the lack of digital subtraction angiography (DSA) for comparison. DSA requires hospitalization and intra-arterial injection of iodinated contrast. Therefore, CE-MRA is considered as an alternative reference to examine the performance of non-contrast MRA techniques. The main objective of this study was to improve the time-efficiency of carotid MRA by combining IPH imaging and MRA into one scan. The agreement with CE-MRA was considered important. Theoretically, both SNAP and CE-MRA remain subject to flow-induced dephasing. Further comparison with a gold standard such as DSA is needed to test if non-invasive imaging workup can be used as an alternative to DSA in clinical practice.

In conclusion, SNAP imaging provides high lumen-wall contrast which can be leveraged to generate large-coverage angiograms for measuring carotid stenosis using the NASCET criteria. Preliminary results demonstrated high reader consistency and high agreement with CE-MRA in asymptomatic subjects with mostly mild to moderate stenosis. Further evaluation in symptomatic and/or high-grade stenosis populations is warranted.

Acknowledgments

Grant Support: This study was supported by the National Institutes of Health (R01 HL103609 and R01 NS083503) and the National Natural Science Foundation of China (81570462), and also with resources and the use of facilities at the VA Puget Sound Health Care System, Seattle, WA, U.S. The contents are solely the responsibility of the authors and do not necessarily represent the official views of the National Institutes of Health, the U.S. Department of Veterans Affairs, or the United States Government.

References

1. Michel JB, Virmani R, Arbustini E, Pasterkamp G. Intraplaque haemorrhages as the trigger of plaque vulnerability. Eur Heart J. 2011; 32:1977–1985. 1985a, 1985b, 1985c. [PubMed: 21398643]
2. Takaya N, Yuan C, Chu BC, et al. Presence of intraplaque hemorrhage stimulates progression of carotid atherosclerotic plaques: a high-resolution magnetic resonance imaging study. Circulation. 2005; 111:2768–2775. [PubMed: 15911695]
3. Sun J, Underhill HR, Hippe DS, Xue Y, Yuan C, Hatsukami TS. Sustained acceleration in carotid atherosclerotic plaque progression with intraplaque hemorrhage: a long-term time course study. J Am Coll Cardiol Img. 2012; 5:798–804.
4. Saam T, Hetterich H, Hoffmann V, et al. Meta-analysis and systematic review of the predictive value of carotid plaque hemorrhage on cerebrovascular events by magnetic resonance imaging. J Am Coll Cardiol. 2013; 62:1081–1091. [PubMed: 23850912]
5. Hosseini AA, Kandiyil N, Macsweeney ST, Altaf N, Auer DP. Carotid plaque hemorrhage on magnetic resonance imaging strongly predicts recurrent ischemia and stroke. Ann Neurol. 2013; 73:774–784. [PubMed: 23463579]
6. Moody AR, Singh N. Incorporating Carotid Plaque Imaging into Routine Clinical Carotid Magnetic Resonance Angiography. Neuroimaging Clin N Am. 2016; 26:29–44. [PubMed: 26610658]

7. Gupta A, Gialdini G, Lerario M, et al. Magnetic resonance angiography detection of abnormal carotid artery plaque in patients with cryptogenic stroke. J Am Heart Assoc. 2015; 4:e2012.
8. Bitar R, Moody AR, Leung G, et al. In vivo 3D high-spatial-resolution MR imaging of intraplaque hemorrhage. Radiology. 2008; 249:259–267. [PubMed: 18796681]
9. Zhu DC, Ferguson MS, DeMarco JK. An optimized 3D inversion recovery prepared fast spoiled gradient recalled sequence for carotid plaque hemorrhage imaging at 3. 0 T. Magn Reson Imaging. 2008; 26:1360–1366. [PubMed: 18583079]
10. Ota H, Yarnykh VL, Ferguson MS, et al. Carotid intraplaque hemorrhage imaging at 3. 0-T MR imaging: comparison of the diagnostic performance of three T1-weighted sequences. Radiology. 2010; 254:551–563. [PubMed: 20093526]
11. Barnett HJM, Taylor DW, Eliasziw M, et al. Benefit of Carotid Endarterectomy in Patients with Symptomatic Moderate or Severe Stenosis. New Engl J Med. 1998; 339:1415–1425. [PubMed: 9811916]
12. Rothwell PM, Eliasziw M, Gutnikov SA, et al. Analysis of pooled data from the randomised controlled trials of endarterectomy for symptomatic carotid stenosis. Lancet. 2003; 361:107–116. [PubMed: 12531577]
13. Rubin MN, Barrett KM, Brott TG, Meschia JF. Asymptomatic carotid stenosis: What we can learn from the next generation of randomized clinical trials. JRSM Cardiovasc Dis. 2014; 3:399039371.
14. Wang J, Bornert P, Zhao H, et al. Simultaneous noncontrast angiography and intraPlaque hemorrhage (SNAP) imaging for carotid atherosclerotic disease evaluation. Magn Reson Med. 2013; 69:337–345. [PubMed: 22442116]
15. Wardlaw JM, Chappell FM, Best JJ, Wartolowska K, Berry E. Non-invasive imaging compared with intra-arterial angiography in the diagnosis of symptomatic carotid stenosis: a meta-analysis. Lancet. 2006; 367:1503–1512. [PubMed: 16679163]
16. Debrey SM, Yu H, Lynch JK, et al. Diagnostic accuracy of magnetic resonance angiography for internal carotid artery disease: a systematic review and meta-analysis. Stroke. 2008; 39:2237–2248. [PubMed: 18556586]
17. Sun J, Canton G, Balu N, et al. Blood Pressure Is a Major Modifiable Risk Factor Implicated in Pathogenesis of Intraplaque Hemorrhage: An In Vivo Magnetic Resonance Imaging Study. Arterioscler Thromb Vasc Biol. 2016; 36:743–749. [PubMed: 26848155]
18. Balu N, Yarnykh VL, Chu B, Wang J, Hatsukami T, Yuan C. Carotid plaque assessment using fast 3D isotropic resolution black-blood MRI. Magn Reson Med. 2011; 65:627–637. [PubMed: 20941742]
19. Zhao H, Wang J, Liu X, et al. Assessment of Carotid Artery Atherosclerotic Disease by Using Three-dimensional Fast Black-Blood MR Imaging: Comparison with DSA. Radiology. 2015; 274:508–516. [PubMed: 25286322]
20. Rothwell PM, Gibson RJ, Slattery J, Sellar RJ, Warlow CP. Equivalence of measurments of carotid stenosis: a comparison of 3 methods on 1001 angiograms. Stroke. 1994; 25:2435–2439. [PubMed: 7974586]
21. Huston JR, Fain SB, Wald JT, et al. Carotid artery: elliptic centric contrast-enhanced MR angiography compared with conventional angiography. Radiology. 2001; 218:138–143. [PubMed: 11152792]
22. Remonda L, Senn P, Barth A, Arnold M, Lövblad K, Schroth G. Contrast-Enhanced 3D MR Angiography of the Carotid Artery: Comparison with Conventional Digital Subtraction Angiography. Am J Neuroradiol. 2002; 23:213–219. [PubMed: 11847044]
23. Davison, AC., Hinkley, DV. Bootstrap methods and their application. Cambridge: Cambridge University Press; 1997.
24. Gupta A, Mushlin AI, Kamel H, Navi BB, Pandya A. Cost-Effectiveness of Carotid Plaque MR Imaging as a Stroke Risk Stratification Tool in Asymptomatic Carotid Artery Stenosis. Radiology. 2015; 277:763–772. [PubMed: 26098459]
25. Nederkoorn PJ, Elgersma OE, van der Graaf Y, Eikelboom BC, Kappelle LJ, Mali WP. Carotid artery stenosis: accuracy of contrast-enhanced MR angiography for diagnosis. Radiology. 2003; 228:677–682. [PubMed: 12869686]

26. U-King-Im JMKS, Trivedi RA, Cross JJ, et al. Measuring Carotid Stenosis on Contrast-Enhanced Magnetic Resonance Angiography. Stroke. 2004; 35:2083–2088. [PubMed: 15243149]

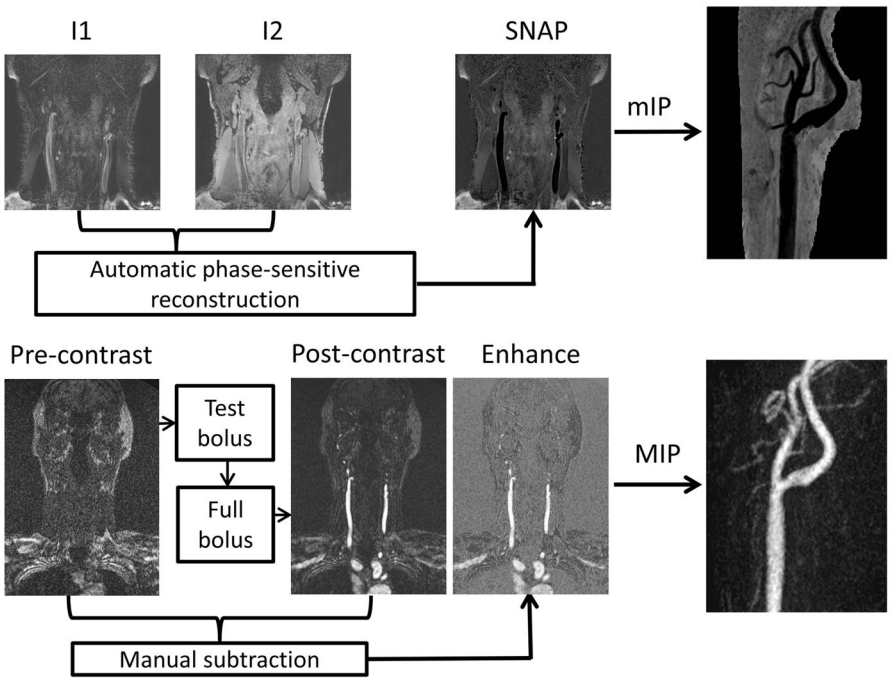

Figure 1.

Comparison between SNAP and CE-MRA. (A) In SNAP (upper panel), inversion recovery (I1, heavily T1-weighted) and reference (I2, proton-density-weighted) images are simultaneously acquired (interleaved scheme). Phase-sensitive reconstruction restores the polarity of MR signals and generates the SNAP data set automatically after SNAP imaging. Minimum intensity projection (mIP) gives angiogram-like images for viewing and measuring luminal stenosis using NASCET criteria. In CE-MRA (lower panel), the sequence is performed twice to acquire pre- and post-contrast mages. Subtraction of pre- and post-contrast image volumes leaves pure enhancement signals, which can be used to generate angiogram-like images through maximum intensity projection (MIP). (B) Reconstructed axial SNAP images and their locations on SNAP MRA show IPH (white arrows) in the presence of mild stenosis.

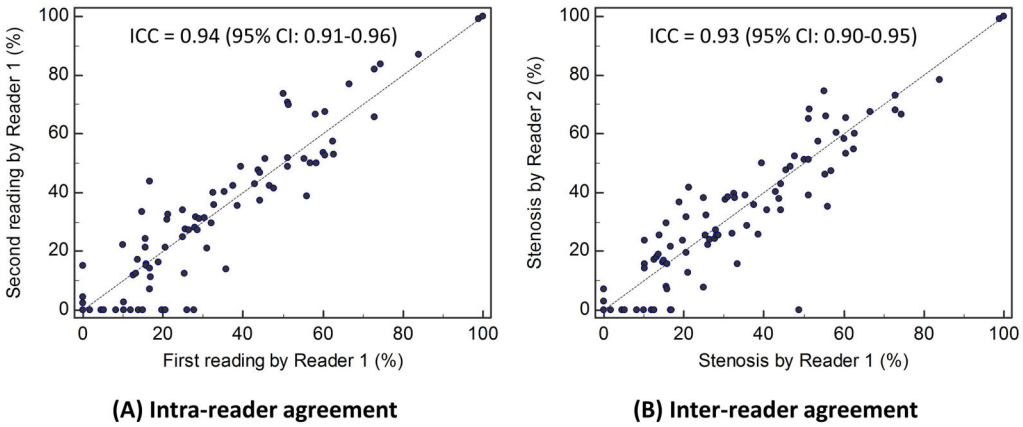

Figure 2.

Reader agreement on quantitative carotid stenosis measurements using SNAP. ICC indicates intra-class correlation coefficient; CI, confidence interval.

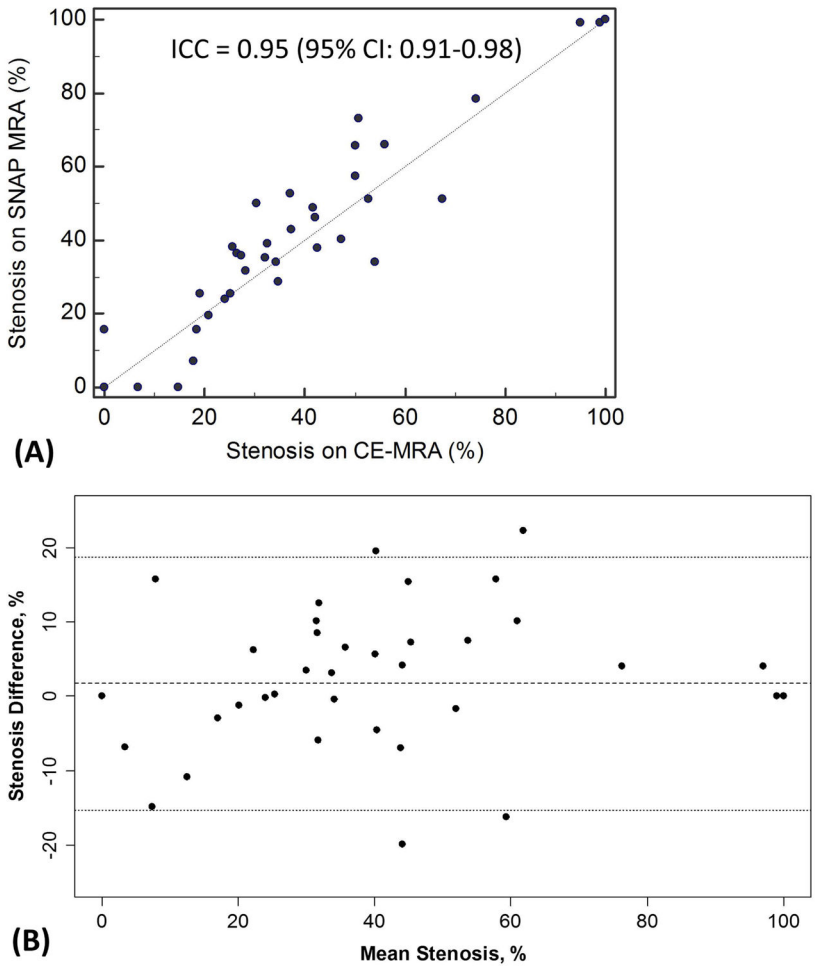

Figure 3.

Agreement between SNAP and CE-MRA. (A) Scatter plot of stenosis measurements made on SNAP and CE-MRA. (B) Bland-Altman plot showing the difference (SNAP minus CE-MRA) versus mean between SNAP and CE-MRA measurements. The dashed line is the mean difference and the dotted lines are limits of agreement. ICC indicates intra-class correlation coefficient.

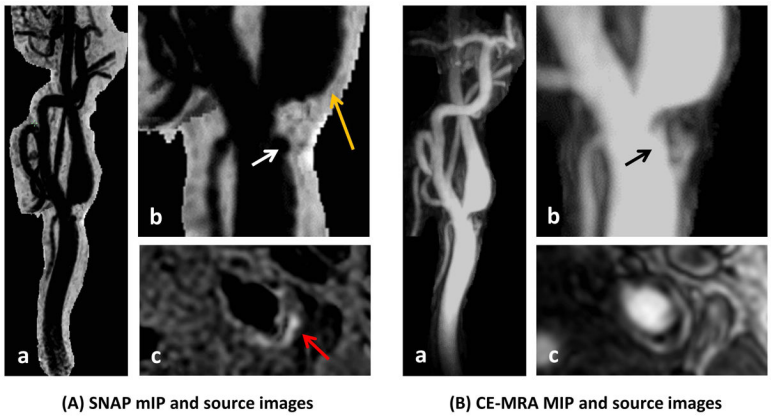

Figure 4.

Carotid bifurcation plaque shown on SNAP MRA (A) and CE-MRA (B). Note the conspicuous lumen boundaries on SNAP minimum intensity projection (mIP) images right after the stenosis where turbulent flow is expected (A-b, orange arrow). Also observed are surface ulceration (white and black arrows) and IPH (A-c, red arrow).

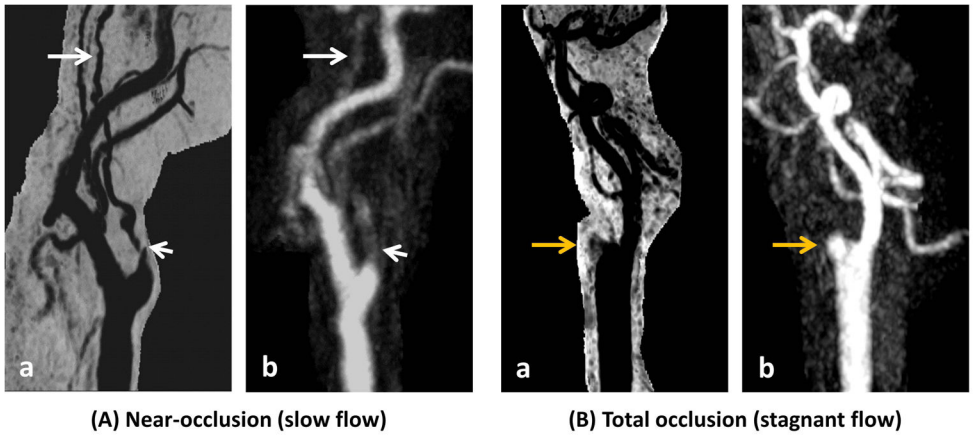

Figure 5.

Near occlusion (A) and total occlusion (B). (A) Shortly after the carotid bifurcation, reduced opacification is seen for an extended segment on CE-MRA (A-b, short arrow), indicating tight stenosis and collapse of distal internal carotid artery. Slow flow is expected. Lumen boundaries remain conspicuous on SNAP MRA (A-a). A signal void (A-a, short arrow) with collapse of the distal segment (A-a, long arrow) is seen. (B) A stub of the internal carotid artery is seen without distal flow on CE-MRA (B-b, orange arrow), consistent with total occlusion of internal carotid artery. A similar finding is seen on SNAP MRA (B-a, orange arrow).

Table 1

Clinical characteristics.

Clinical variables	Mean ± SD or n (%)	Range
Sex		
Male	40 (69.0)	
Female	18 (31.0)	
Age, years	71 ± 7	(55 – 85)
Body mass index – kg/m2	28 ± 7	(18 – 58)
Smoking	7 (12.1)	
Hypertension	44 (75.9)	
Hyperlipidemia	52 (89.7)	
Diabetes	6 (10.3)	
Coronary artery disease	19 (32.8)	
Cerebrovascular disease	17 (29.3)	
Peripheral artery disease	16 (27.6)	
Statin therapy	47 (81.0)	
Antiplatelet/anticoagulant therapy	46 (79.3)	

Table 2

Comparing stenosis grades between SNAP and CE-MRA.

SNAP	CE-MRA			
	0–29%	**30–69%**	**70–99%**	**100%**
0–29%	22	1	0	0
30–69%	4	16	0	0
70–99%	0	1	3	0
100%	0	0	0	1